
Article:
Harman-Thomas, J.M., Kashif, T.A., Hughes, K.J. et al. (2 more authors) (2023) Experimental and modelling study of hydrogen ignition in CO2 bath gas. Fuel, 334 (Part 1). 126664. ISSN 0016-2361

https://doi.org/10.1016/j.fuel.2022.126664

Experimental and Modelling Study of Hydrogen Ignition in CO_2 Bath Gas

James M. Harman-Thomas[1,+], Touqeer Anwar Kashif[2,+], Kevin J. Hughes[1], Mohamed Pourkashanian[1], Aamir Farooq[2,*]

[1]*The University of Sheffield, Department of Mechanical Engineering, Energy 2050, Sheffield, United Kingdom*
[2]*Clean Combustion Research Center, King Abdullah University of Science and Technology (KAUST), Thuwal 23955, Saudi Arabia*

*Corresponding author email: aamir.farooq@kaust.edu.sa

+Both Authors Contributed Equally

Abstract

Direct-fired supercritical CO_2 power cycles, operating on natural gas or syngas, have been proposed as future energy technologies with 100% carbon capture at a price competitive with existing fossil fuel technologies. Likewise, blue or green hydrogen may be used for power generation to counter the intermittency of renewable power technologies. In this work, ignition delay times (IDTs) of hydrogen were measured in a high concentration of CO_2 bath gas over 1050 – 1300 K and pressures between 20 and 40 bar. Measured datasets were compared with chemical kinetic simulations using AramcoMech 2.0 and the University of Sheffield supercritical CO_2 (UoS sCO_2 2.0) chemical kinetic mechanisms. The UoS sCO_2 2.0 mechanism was recently developed to model IDTs of methane, hydrogen, and syngas in CO_2 bath gas. Sensitivity analyses were used to identify important reactions and to illustrate the trends observed among various datasets. The performance of both mechanisms was evaluated quantitively by comparing the average absolute error between the predicted and experimental IDTs, which showed UoS sCO_2 2.0 as the superior mechanism for modelling hydrogen IDTs in CO_2 bath gas. The importance of OH time-histories is identified as the most appropriate next step in further validation of the kinetic mechanism.

Keywords: *Supercritical CO_2; Hydrogen; Ignition Delay Time; Shock Tube; Chemical Kinetics*

1. Introduction

The IPCC's Sixth Assessment Report (2021) revealed that anthropogenic activities have caused a global surface temperature rise of 1.07 °C from 1850-1900 to 2010-2019 [1]. The increase in global temperatures and the resulting climate change has led to an increase in the frequency and intensity of extreme weather events worldwide. In 2019 alone, there were 396 global disasters worldwide, affecting 95 million people and costing nearly US$130 billion [2]. As of 2021, 131 countries have announced or adopted policies to become net-zero by 2060 or earlier [3]. However, it is extremely unlikely that our reliance on fossil fuels will disappear anytime soon, implying that methods of utilizing fossil fuels without releasing harmful emissions into the atmosphere will be required to meet these targets.

Direct-fired supercritical CO_2 (sCO_2) combustion cycles have the potential for 100% inherent carbon capture at a price competitive with existing fossil fuel technology [4]. Direct-fired sCO_2 cycles operate above 300 atm with a 96% dilution of carbon dioxide (CO_2), above its critical pressure and temperature, where it becomes supercritical and possesses properties of both a liquid and a gas [4]. The Allam-Fetvedt cycle is the most established direct-fired sCO_2 cycle, with an operational 50 MW pilot plant [5], and two 280 MW plants in the US and one 300 MW plant under development in the UK [6, 7]. The combustion chamber of the Allam-Fetvedt cycle has a predicted generation efficiency of 53.9% for natural gas combustion [8]. Burning natural gas and pure oxygen, produced from an onsite air separation unit, produces water and CO_2 as the only products of combustion. These can be easily separated via the condensation of water to produce a high-purity stream of CO_2 which can be sequestered or used in various chemical conversion processes.

One current challenge faced by the Allam-Fetvedt cycle is the lack of a reliable chemical kinetic mechanism that can accurately model combustion at high pressures with a large dilution of CO_2. Most of the available experimental data have been measured at lower pressures and with a smaller mole fraction of CO_2. Recently, the University of Sheffield Supercritical CO_2 Mechanism (UoS sCO_2 Mech) [9] was

developed using literature ignition delay time (IDT) data of methane, hydrogen (H_2) and syngas over a range of pressures and CO_2 dilutions. This work identified a need for further H_2 IDT measurements as few (only three) datasets are available at relevant conditions. Shao et al. [10] studied IDTs of H_2 with 85% CO_2 dilution at approximately 38, 110 and 271 bar. Interestingly, the investigated chemical kinetic mechanisms showed a better agreement with the higher pressure datasets than at 38 bar [9]. Therefore, IDT data between 20 and 40 bar at various equivalence ratios and CO_2 dilutions are needed to validate and improve the performance of chemical kinetics mechanisms at these conditions.

The current work is aimed at obtaining new IDT data for H_2 ignition in a high concentration of CO_2 bath gas. Ignition delays were measured at high temperatures and 20-40 bar pressures with variable bath gas compositions (N_2, CO_2). The datasets were subsequently compared with predictions of UoS sCO_2 Mech and AramcoMech 2.0 to evaluate their performance in modelling CO_2-diluted H_2 ignition.

2. Experimental Details

Ignition delays of hydrogen were measured in the high-pressure shock tube (HPST) facility at King Abdullah University of Science and Technology (KAUST). The HPST is constructed from stainless steel capable of withstanding pressures up to 300 bar. The driven section is 6.6 m long with a circular cross-sectional diameter of 10.16 cm. The driver section is modular and can be extended up to 6.6 m. It houses a double diaphragm arrangement which allows for better shock-to-shock repeatability. Further details of the facility may be found elsewhere [11-13].

Incident shock speed was measured by six PCB 113B26 piezoelectric pressure transducers (PZTs), placed axially along the last 3.6 m of the driven section. Ideal Rankine-Hugonoit shock relations were used to calculate thermodynamic conditions (P_5 and T_5) behind reflected shock waves with uncertainties of <1%. Ideal gas relations were used here as Shao et al. [10] showed that there is a negligible difference in post-shock conditions calculated using real gas equations of state. Incident shock attenuation rates

varied from 0.5 to 1.8%/m. An uncertainty value of 15% and 20% is reported for IDT measurements in N_2 and CO_2 containing mixtures, respectively.

Table 1. IDT mixtures studied in this work and the results of quantitative comparisons.

Mix.	Species Mole Fraction				Mixture Conditions			Average Absolute Error (*E*) (%)	
	H_2	O_2	N_2	CO_2	T [K]	P [bar]	ϕ	AramcoMech 2.0	UoS sCO_2 2.0
1	10	5	35	50	1103-1243	20.5-21.7	1.0	40.9	3.1
2	10	5	-	85	1142-1261	18.5-19.6	1.0	50.0	11.8
3	10	5	85	-	1059-1214	19.2-20.5	1.0	13.6	18.2
4	12	3	35	50	1123-1238	20.2-21.0	2.0	11.4	22.4
5	4.3	10.7	35	50	1162-1255	19.4-19.9	0.2	59.5	29.0
6	5	10	-	85	1204-1302	42.0-43.0	0.25	17.0	14.4
7	7.5	7.5	-	85	1164-1300	41.4-42.1	0.5	7.8	18.1
8	10	5	-	85	1123-1266	40.5-41.6	1.0	24.4	11.6
Average *E* (%)								28.1	16.1

Sidewall pressure was monitored using a Kistler 603B1 PZT and OH* chemiluminescence signals were measured at the endwall and sidewall through photomultiplier tubes (PMTs). Mixtures were prepared in a 20 L stainless steel vessel equipped with a magnetic stirrer. Research grade (99.999%) gases were used, and each mixture was given sufficient time to mix before experiments to ensure homogeneity. Table 1 shows the compositions of the 8 mixtures investigated along with the reflected-shock temperature and pressure ranges. These mixture compositions were selected to fill in the gaps in literature IDT datasets of hydrogen over 20 – 40 bar and to investigate the effect of varying CO_2 bath gas composition equivalence ratio. A kinetic mechanism should be able to accurately simulate combustion at lower pressures before expanding to the higher pressures of the Allam-Fetvedt cycle.

2.1. Identification of Time Zero

Time zero identification is challenging for mixtures with high levels of CO_2 dilution, as has been reported in literature shock tube studies [14, 15]. Non-idealities from CO_2 dilution mainly originate due to the

63 interaction of the reflected shock wave (RSW) with an energy-deficient boundary layer behind the incident
64 shock wave (ISW), thus leading to the bifurcation of the reflected shock. An oblique shock will then
65 precede the normal shock near the boundaries, thus altering the state of gas in region 5 (i.e., behind the
66 RSW) [16-18]. These alterations are more pronounced in regions further from the endwall. Such fluid
67 disturbances manifest themselves in the pressure profiles at endwall and sidewall transducers.

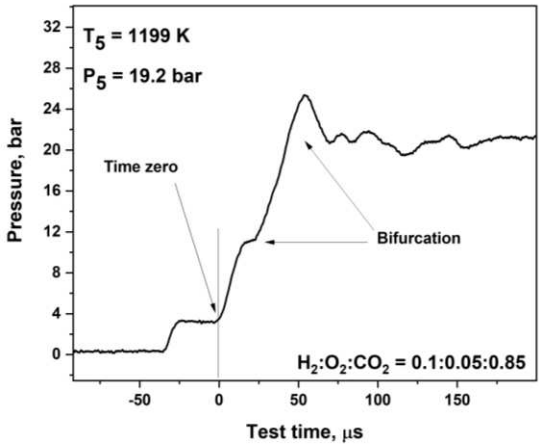

68

69 Fig. 1. Sidewall pressure history for a representative experiment of 85% CO_2 diluted H_2 mixture.

70 Hargis et al. [14] compared sidewall and endwall pressure histories at various CO_2 dilutions for methane
71 mixtures, and highlighted the superiority of endwall pressure profiles for time zero determination. Due to
72 the lack of an endwall pressure transducer in the present work, measurements were made with a sidewall
73 Kistler transducer located just 10.48 mm from the endwall. In contrast to the usual practice where time
74 zero is defined as the midpoint of the reflected shock wave, time zero is defined in this work at the start
75 of reflected shock pressure rise. This is based on inferences from the pressure traces of Hargis et al. [14]
76 and Karimi et al. [15]. Figure 1 shows a representative sidewall pressure trace for an 85% CO_2-diluted H_2
77 mixture at 20 bar from the present work. The extent of bifurcation is significantly smaller than in Hargis
78 et al. [14] experiments, and this is likely due to their sidewall pressure transducer being further away (16
79 mm) from the endwall.

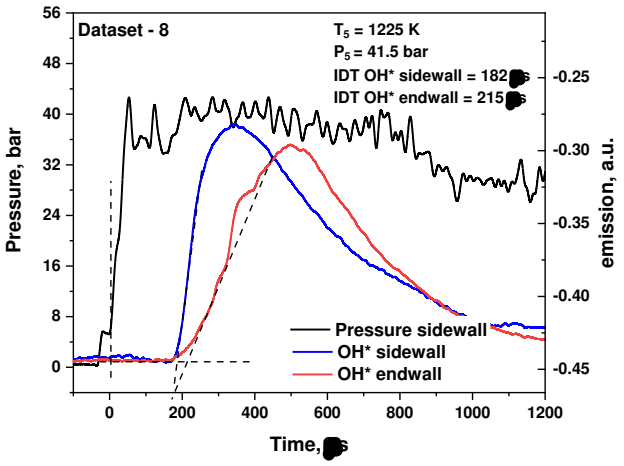

Fig. 2. Representative profiles for IDT measurements of dataset 8 (H_2:O_2:CO_2=10:5:85) at 1225 K.

2.2. Determination of Ignition Delay

In an ideal scenario with a homogenous temperature and pressure field behind the reflected shock wave, the mixture is expected to ignite near the endwall as the gas there is exposed to high-temperature conditions for a longer duration compared to the gas further away from the endwall. The onset of ignition is determined as the time of intersection of the baseline OH* emission with the tangent of the steepest rise of OH* emissions, as shown in Fig. 2. This method gives more representative IDTs for endwall measurements in CO_2 bath gas compared to the maximum gradient of OH* profile. A similar method to ours was used by Karimi et al. [15] who defined the onset of ignition as the onset of OH* emission signal rise. These methods would give very similar IDTs in ideal conditions [19].

At high levels of CO_2 dilution, small hot spots can develop as a result of interactions between the RSW and the boundary layer [20]. These hot spots alter the homogeneity of the mixture and can potentially cause an early initiation of the ignition process which can lead to a false interpretation of IDTs from pressure and emission traces. For the present mixtures, a noticeable early rise of OH* sidewall emission was observed, as can be seen in Fig. 2. Similar observations were reported by Karimi et al. [15] for heavily diluted CO_2 mixtures. They associated the hotspots formed in the periphery of the shock tube to the increased bifurcation in these mixtures. The small ignition kernels are picked up by the sidewall OH*

earlier than the endwall emission. The large internal diameter of the shock tube ensures that the core of the mixture remains unaffected, as reported by Karimi et al. [15]. Endwall emission thus responds to the ignition of the core gas as it sees the bulk of the volume [19].

Therefore, in this work, the onset of ignition was determined through the maximum slope of the OH* endwall emission trace. A comparison of IDTs for H_2 dataset 6 (5% H_2/10% O_2/ 85% CO_2) against a dataset from Shao et al. [10] is shown in Fig. 3. The two datasets are in relatively good agreement at lower temperatures. The disagreement in the datasets at a higher temperature may be explained by the high uncertainty of IDTs smaller than 100 µs due to the uncertainty in identifying time zero. The discrepancy seen between the present data and that of Shao et al. [10] is likely down to the different methods of IDT determination. Shao et al. [10] used sidewall emissions, which as discussed, is more sensitive to the early-onset ignition, explaining the smaller value of their measured IDT compared to the endwall IDT from the present study. Uncertainty in our measured ignition delay times is estimated to be +/- 20% (see Supplementary Material).

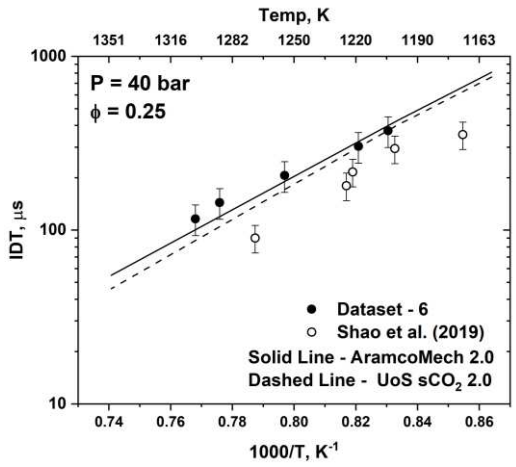

Fig. 3. Comparison of mixture 6 (H_2:O_2:CO_2=5:10:85) IDTs with literature data [10]. IDTs from the current work (Dataset – 6) were obtained using endwall OH* emission, while Shao et al. used sidewall OH* emission.

3. Modelling Procedure

IDTs were modelled using Chemkin-Pro (zero-D batch reactor, constant UV) with two chemical kinetic mechanisms, namely AramcoMech 2.0 [21] and UoS sCO_2 2.0 [9]. An experimentally determined

2.5%/ms dp/dt was incorporated in the simulations to account for the gradual pressure increase behind the RSW. Similar to the experimental procedure, IDT was determined using the simulated OH time-history profile. The rate coefficients in the UoS sCO_2 2.0 mechanism were chosen based on a combination of recent reports, method of determination and how they affected the prediction of 52 IDT datasets [9].

A normalized OH sensitivity analysis at the point of ignition was performed to compare the performances of the two mechanisms and identify the reactions most sensitive to IDT prediction at different conditions. A positive OH sensitivity coefficient indicates that an increase in the rate of reaction will reduce IDT (increase reactivity), and vice versa. The performance of the two mechanisms was compared using Eq. (1), which calculates an average absolute error (*E, %*) between the experimental and simulated IDTs [9].

Eq. (1) $$E(\%) = \frac{1}{N}\sum_{i=1}^{N}\left|\frac{IDT_{sim,i}-IDT_{exp,i}}{IDT_{exp,i}}\right| \times 100$$

Here, N is the number of data points in a dataset. $IDT_{sim,i}$ and $IDT_{exp,i}$ are the simulated and experimental data points, respectively, for the ith data point. The average absolute error value is a good way to compare the mechanism performance across a large number of datasets, where a smaller E value, ideally within the experimental uncertainty, indicates a better performance.

Only a single modification was made for the creation of UoS sCO_2 2.0 from the original publication [9]. The third body efficiency of CO_2 was increased from 2.0 to 3.8 in Reaction 1. This change was found to lead to large improvements in the performance of the mechanism for this study without adversely affecting the simulations of datasets used to develop the original mechanism [9]. The importance of Reaction 1 to H_2 combustion is discussed further in Section 4.

Reaction 1. $H + O_2 (+M) \rightleftharpoons HO_2 (+M)$

4. Results and Discussion

Eight H_2 IDT datasets were measured in this study to allow for mechanism investigation and comparison over a range of experimental conditions. In the following, discussion and analysis are split in two key

domains. Firstly, the effect of altering CO_2 dilution is considered in Section 4.1, followed by the effect of altering the equivalence ratio in Section 4.2. The results of the quantitative analysis, using Eq. (1), are presented in Table 1.

4.1. Effect of CO_2 Dilution

Datasets 1, 2 and 3 investigated IDTs of stoichiometric H_2 in 85% dilution of three different bath gases. Dataset 1 was composed of 50% CO_2 and 35% N_2, whilst Datasets 2 and 3 contained 85% CO_2 and 85% N_2, respectively. These datasets are shown in Fig. 4 and compared with the predictions of AramcoMech 2.0 and UoS sCO_2 2.0.

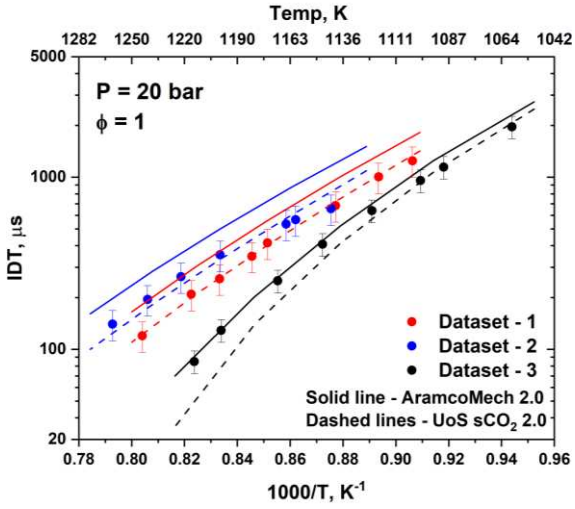

Fig. 4. Comparison of IDTs of datasets 1 (H_2:O_2:N_2:CO_2=10:5:35:50), 2 (H_2:O_2:CO_2=10:5:85) and 3 (H_2:O_2:N_2=10:5:85) with AramcoMech 2.0 and UoS sCO_2 2.0.

It may be seen in Fig. 4 that as CO_2 dilution is increased, mixture reactivity is decreased (longer IDTs). Ignition delays are longer in CO_2 bath gas due to the smaller rate of OH production. This is due to the branching of H + O_2 reaction between chain propagation (Reaction 1) and chain branching (Reaction 2), which favours chain propagation for a larger concentration of CO_2. Additionally, CO_2 consumes H radicals via the reverse of Reaction 3 to form CO and OH. This reaction competes with Reaction 2 (forward direction) for H radicals, thus slowing the rate of the branching reaction and reducing the production of

158 OH radicals. Interestingly, Karimi et al. [15] did not observe any significant difference in IDTs of syngas
159 in CO_2 vs Ar bath gas.

160 **Reaction 2.** $H + O_2 \rightleftharpoons O + OH$

161 **Reaction 3.** $CO + OH \rightleftharpoons CO_2 + H$

162 A key observation is the convergence of the three datasets at lower temperatures in Fig. 4. This is not
163 modelled well by both mechanisms, particularly for datasets 1 and 2. There are two possible explanations
164 for this. Either the mechanisms lack some chemistry required to model the low-temperature IDTs or the
165 longest IDT measured for dataset 3 (85% CO_2) suffered from premature ignition because of
166 inhomogeneities, for example, due to shock bifurcation. Longer IDTs get affected more from bifurcation
167 as the hot spots associated with bifurcation have enough time to induce localized ignition events [22].
168 Therefore, for CO_2 diluted mixtures longer IDTs were limited by the bifurcation growth time scale (500
169 μs) as given by Gordon and Ihme [22].

170 Figure 4 and the quantitative analysis in Table 1 show that UoS sCO_2 2.0 gives better predictions for
171 datasets 1 and 2 which contain CO_2 dilution, whereas AramcoMech 2.0 performs better for dataset 3 which
172 only contains N_2 bath gas. For dataset 3 (85% N_2), whilst both mechanisms predict the four lowest
173 temperature measurements within the 15% experimental error, UoS sCO_2 2.0 shows a relatively poor
174 agreement with the three highest temperature data points. To analyze this disagreement, Fig. 5 shows
175 normalized OH sensitivity analysis of dataset 3 (85% N_2) at 1050 and 1200 K. At the higher temperature
176 where the agreement is poor, there are only two reactions (Reactions 1 and 2) with a relatively large
177 sensitivity coefficient. These are the two possible pathways of $H + O_2$ reaction.

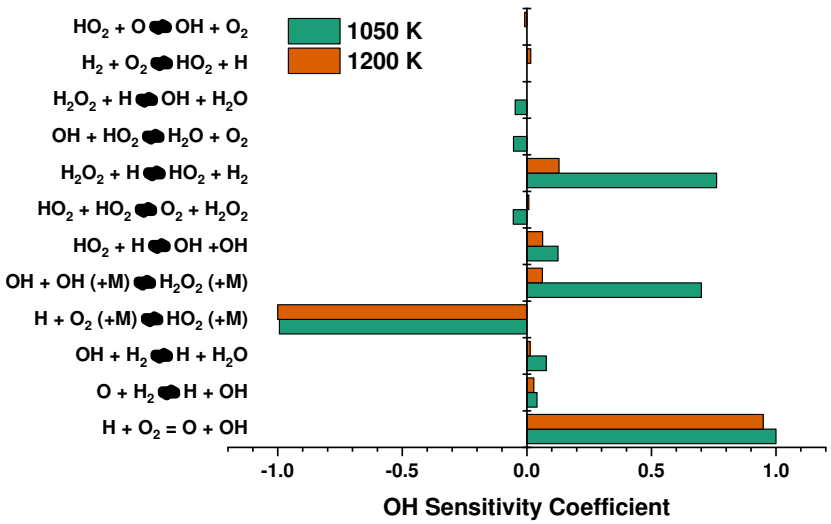

178

179 Fig. 5. Normalized OH sensitivity analysis of dataset 3 (H_2:O_2:N_2=10:5:85) for UoS sCO_2 2.0 at 1050 and 1200 K.

180 It is noted that the steep gradient on the predictive curve of dataset 3 is likely due to the temperature
181 coefficient (*n*) of the rate coefficient of Reaction 2. Even a small alteration of -0.01 had a large effect on
182 the predictions near the highest temperature data points of datasets 1-3. However, such a change to the
183 rate coefficient was not made just to fit one dataset. Secondly, Reaction 2 has been investigated thoroughly
184 by the combustion community [23, 24]. Due to the importance of Reactions 1 and 2 to high-pressure
185 hydrogen and syngas [15] combustion in CO_2, it is suggested that the rate coefficient of Reaction 1 be
186 studied in CO_2 bath gas [25, 26] for accurate determination of the third body efficiency of CO_2.

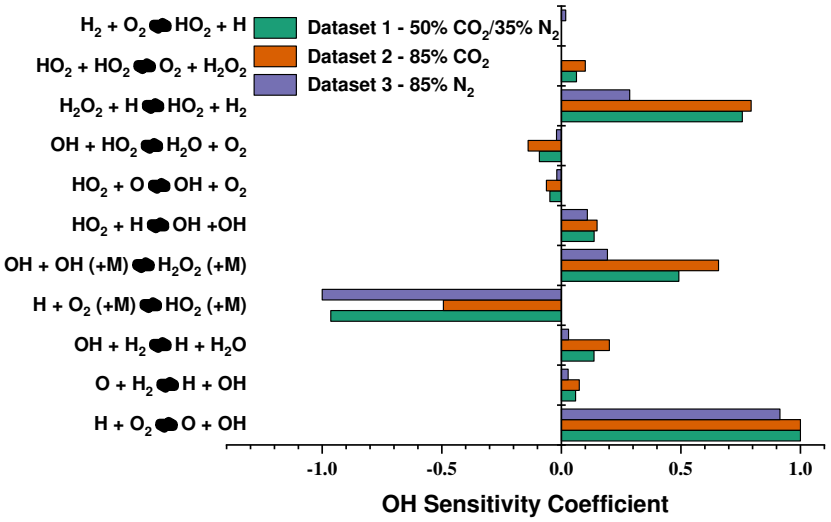

187

Fig. 6. Normalized OH sensitivity analysis of datasets 1 (H_2:O_2:N_2:CO_2=10:5:35:50), 2 (H_2:O_2:CO_2=10:5:85) and 3 (H_2:O_2:N_2=10:5:85) for UoS sCO_2 2.0 at 1150 K.

Figure 6 compares OH sensitivity analyses of datasets 1-3. A key point to note in Fig. 6 is the greater similarity of the sensitivity coefficients of 50% CO_2/ 35% N_2 blend mixture to 85% CO_2 mixture, in contrast to the sensitivity coefficients of 85% N_2 mixture. Further to this, there is a significant overlap of the IDTs of datasets 1 and 2 (see Fig. 4) despite a 35% difference in the bath gas composition, and this trend is predicted by both kinetic mechanisms. The reason for this convergence of IDTs as the concentration of CO_2 increases is likely due to the chemical effect of CO_2 competing for H radicals via Reaction 3. This effect is non-linear, and 50% CO_2 leads to a sharp increase in CO mole fraction, whereas the subsequent 35% addition has a smaller effect on the maximum CO mole fraction and the percentage of H radicals consumed by Reaction 3 remains similar; therefore, the increase in IDTs isn't as pronounced.

Furthermore, there are key differences in the radical pool at the point of ignition when combusting in 85% CO_2. Figure 7 shows the maximum concentration of selected species for three different bath gas compositions (85% CO_2, 50% CO_2, 85% N_2) studied at 20 bar and 1200 K. Clearly, CO formation only occurs in CO_2 containing mixtures due to Reaction 3, but this also consumes H radical and, therefore, reduces its maximum concentration. Interestingly, the maximum OH radical concentration is much greater in N_2 relative to CO_2, despite Reaction 3 leading to OH formation. Conversely, the concentration of HO_2 is much greater in CO_2 bath gas due to the depleted H radical pool. In 85% N_2, more OH is formed through Reaction 2 and, subsequently, Reaction 4. Since there is a greater competition for H radicals in CO_2, this reaction pathway is reduced and less OH is formed. Under both conditions, the majority of OH is formed through Reaction 5. Due to the greater concentration of H radicals in N_2, this reaction is faster, leading to more OH production and a faster depletion of HO_2, as shown in Fig. 7.

Reaction 4. $H_2 + O \rightleftharpoons H + OH$

Reaction 5. $HO_2 + H \rightleftharpoons OH + OH$

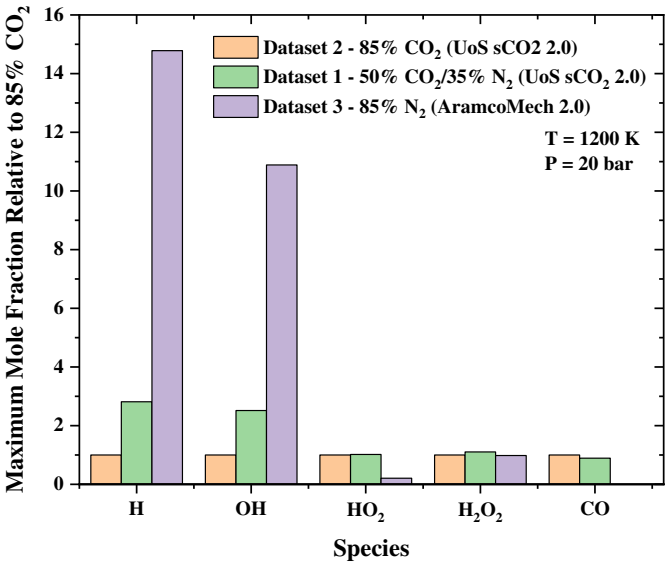

Fig. 7. Maximum species concentrations at the point of ignition for key intermediates relative to Dataset 2 with 85% CO_2 dilution.

These trends suggest that IDT data measured to develop a chemical kinetic mechanism for CO_2 combustion do not need to be done in 100% CO_2 bath gas. As the controlling reactions and IDTs are similar for datasets 1 and 2, measuring datasets at only 50% CO_2 produces results that are just as useful as 85% CO_2. Reduction in the CO_2 concentration helps in lowering non-ideal effects (e.g., bifurcation), as discussed in Section 2, which means that IDTs can be measured with smaller uncertainty and at longer test times. This is not to say that IDT datasets in a pure CO_2 bath gas are not important, but CO_2/N_2 bath gas blends provide a useful benchmark with reduced uncertainty in IDT measurements.

4.2. Effect of Equivalence Ratio

The effect of altering the equivalence ratio for H_2 ignition was investigated with six datasets. Figure 8 displays the effect of increasing the equivalence ratio (ϕ = 0.2, 1, 2) at 20 bar in a bath gas of 50% CO_2 / 35% N_2. Datasets 1 and 4 overlap over the entire temperature range, while dataset 5 (ϕ = 0.2) exhibits slightly longer IDTs at high temperatures. These results are consistent with Hu et al. [27] who observed a similar overlap of hydrogen IDTs in argon bath gas at 16 bar for ϕ = 0.5, 1.0 and 2.0. Sensitivity analysis

in Fig. 9 shows that the three datasets are primarily sensitive to Reactions 1 and 2, and the sensitivity coefficients are almost the same for the three equivalence ratios.

Table 1 shows that the E (%) value for dataset 5 ($\phi = 0.2$) is the largest for both AramcoMech 2.0 and UoS sCO_2 2.0 across all H_2 datasets, thus indicating the difficulty to model IDTs at the lowest equivalence ratio. Interestingly, the performance of AramcoMech 2.0 improves when moving from $\phi = 1.0$ to $\phi = 2.0$, whereas UoS sCO_2 has better agreement at $\phi = 1.0$ compared to $\phi = 2.0$. This is likely due to the strong overlap in Datasets 4 and 5, which is not predicted particularly well by either mechanism.

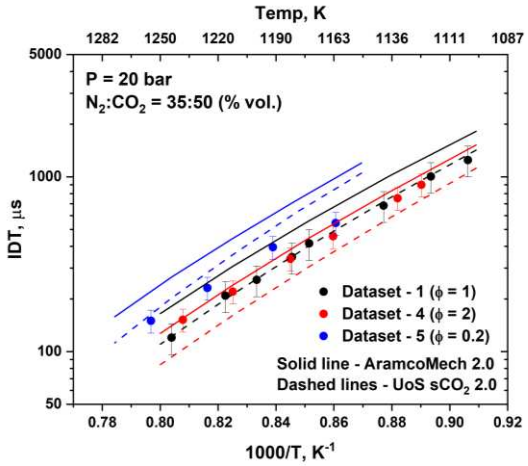

Fig. 8. Comparison of IDTs of datasets 1 (H_2:O_2:N_2:CO_2=10:5:35:50), 4 (H_2:O_2:N_2:CO_2=12:3:35:50) and 5 (H_2:O_2:N_2:CO_2=4.3:10.7:35:50) with AramcoMech 2.0 and UoS sCO_2 2.0.

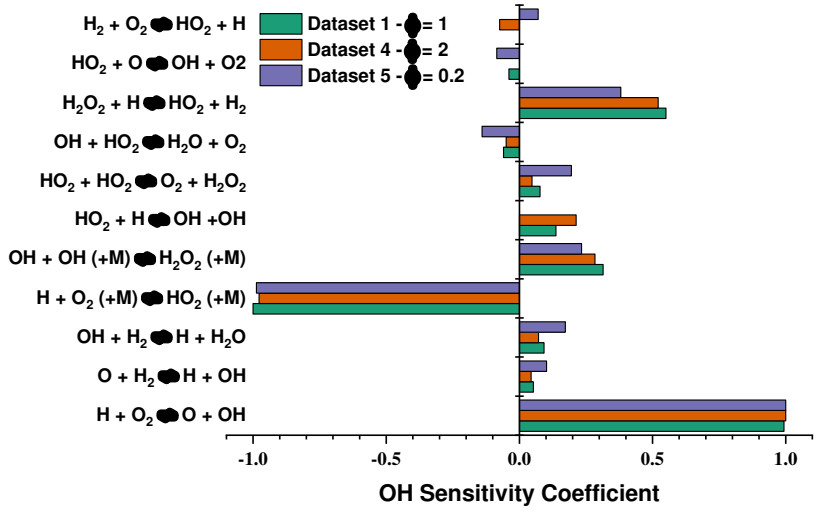

Fig. 9. Normalized OH sensitivity analysis of datasets 1 (H_2:O_2:N_2:CO_2=10:5:35:50), 4 (H_2:O_2:N_2:CO_2=12:3:35:50) and 5 (H_2:O_2:N_2:CO_2=4.3:10.7:35:50) for UoS sCO_2 2.0 at 1200 K.

241 Figure 8 shows that UoS sCO_2 2.0 overpredicts IDTs for dataset 5 ($\phi = 0.2$) while underpredicting dataset
242 4 ($\phi = 2.0$). Sensitivity analysis (Fig. 9) indicates that one possible explanation is Reaction 6, which has
243 opposite sensitivity coefficients for $\phi = 0.2$ and $\phi = 2.0$, and it did not appear in the top sensitive reactions
244 at $\phi = 1.0$.

245 **Reaction 6.** $H_2 + O_2 \rightleftharpoons HO_2 + H$

246 While Reaction 5 is the only reaction that has a significantly higher sensitivity at $\phi = 2.0$ than $\phi = 0.2$,
247 Reactions 7, 8 and 9 have a much larger sensitivity coefficient at $\phi = 0.2$. It may be anticipated that tuning
248 the rate coefficients of these reactions will reduce the effect of equivalence ratio changes on simulated
249 IDTs, and thus lead to the mechanism predictions being in better agreement with the experimental IDTs.
250 This is proposed as one of the possible future routes for mechanism optimization. Nonetheless, it must be
251 noted that except for dataset 4, UoS sCO_2 2.0 significantly outperformed AramcoMech 2.0 in predicting
252 the equivalence ratio dependence.

253 **Reaction 7.** $HO_2 + HO_2 \rightleftharpoons O_2 + H_2O_2$

254 **Reaction 8.** $OH + HO_2 \rightleftharpoons H_2O + O_2$

255 **Reaction 9.** $OH + H_2 \rightleftharpoons H + H_2O$

256 Figure 10 shows the effect of increasing the equivalence ratio ($\phi = 0.25, 0.5, 1$) in 85% CO_2 bath gas for
257 H_2 ignition at 40 bar. In comparison to 20 bar (Fig. 8), the performance of AramcoMech 2.0 is much more
258 competitive. This is surprising as the mechanism was originally validated for relatively low pressures and
259 low CO_2 dilutions. The performance of UoS sCO_2 2.0 is also better at 40 bar than 20 bar. This is likely
260 because the mechanism was primarily validated using three H_2 IDT datasets of Shao et al. [28], where the
261 lowest pressure was ~40 bar with CO_2 dilution of 85% (which is directly comparable with dataset 6 from
262 the current work). This means that UoS sCO_2 2.0 was not validated to model H_2 IDTs below 40 bar. This
263 illustrates the importance of the IDT data reported here in developing a comprehensive chemical kinetic
264 mechanism for modelling sCO_2 combustion. While datasets 6, 7 and 8 shown in Fig. 10 are not directly

comparable to those at 20 bar (Fig. 8) due to the different bath gas composition, the trends observed are very similar. Although the equivalence ratio range is smaller for the three datasets at 40 bar compared to those at 20 bar, there is a large overlap of IDTs (Fig. 10) at the three equivalence ratios with dataset 8 (ϕ = 1.0) being slightly faster. AramcoMech predicts negligible equivalence ratio dependence while UoS sCO_2 predicts a small variation of IDTs with equivalence ratio which is more aligned with the experimental data.

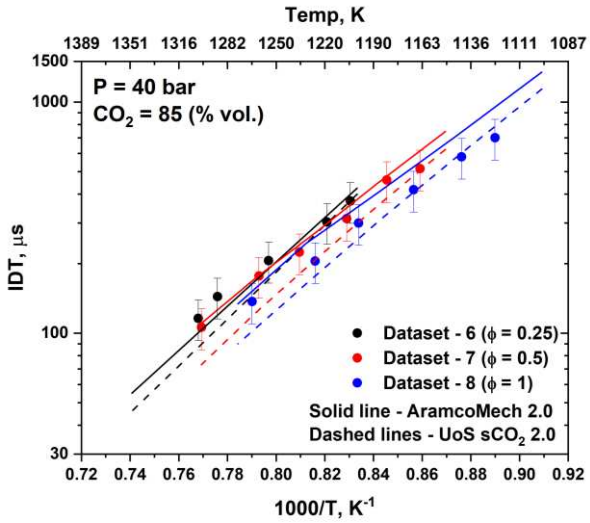

Fig. 10. Comparison of IDTs of datasets 6 (H_2:O_2:CO_2=5:10:85), 7 (H_2:O_2:CO_2=7.5:7.5:85) and 8 (H_2:O_2:CO_2=10:5:85) with AramcoMech 2.0 and UoS sCO_2 2.0.

Figure 11 shows normalized OH sensitivity analysis of datasets 6 and 8 at 1250 K, which is used to visualize the effect of equivalence ratio on H_2 ignition at 40 bar. In Fig. 10, UoS sCO_2 2.0 predicts faster IDTs compared to the experiments at high temperatures. This is likely due to the temperature dependence of Reaction 2, as discussed earlier. Another possible explanation is the overprediction of the rate coefficient of Reaction 10 which has the second-largest positive sensitivity coefficient in Fig. 11. AramcoMech 2.0 and UoS sCO_2 2.0 both use the rate coefficient of Reaction 10 from Ellingson et al. [29], with UoS sCO_2 2.0 having a slightly smaller *A* factor, reduced within the experimental uncertainty [9]. Therefore, there may be a significant effect on the predicted IDTs if the rate coefficient of Reaction 10

was changed to those given by Tsang and Hampson [30] or Wu et al. [31], where both of these studies propose a smaller A factor but a larger temperature coefficient.

Reaction 10. $H_2O_2 + H \rightleftharpoons HO_2 + H_2$

Further experiments at the high and low-temperature ends would be helpful in understanding these discrepancies. Longer test times can be achieved with driver gas tailoring in a shock tube [32] but could be more prone to non-ideal effects. Experiments at shorter test times are challenging due to the larger uncertainty in shock tube measurements below 100 μs.

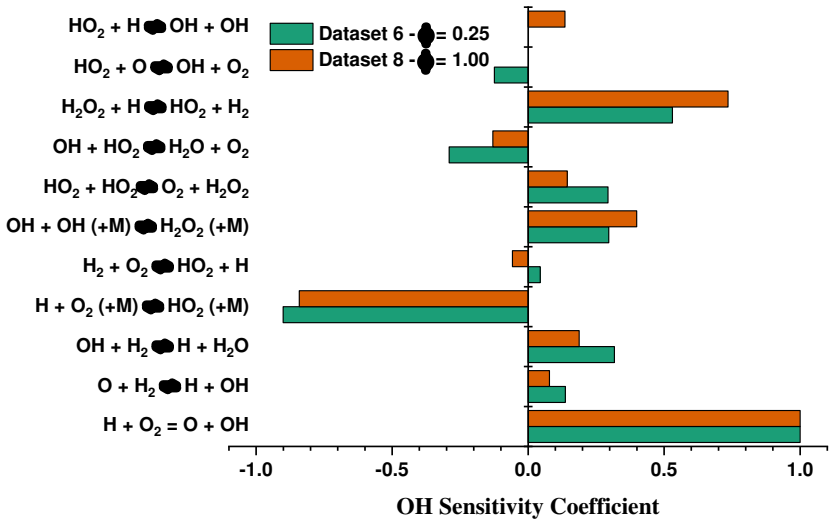

Fig. 11. Normalized OH sensitivity analysis of datasets 6 (H_2:O_2:CO_2=5:10:85) and 8 (H_2:O_2:CO_2=10:5:85) for UoS sCO_2 2.0 at 1250 K.

5. Validation of UoS sCO_2 Mechanism

A key objective of this study is to validate UoS sCO_2 2.0 for predicting IDTs of H_2 in CO_2 bath gas. For the eight H_2 datasets studied here, the average absolute error (E) was determined to be 16.1% for UoS sCO_2 2.0, which is a significant improvement compared to 28.1% of AramcoMech 2.0. In addition, UoS sCO_2 2.0 fits six datasets within a 20% error, which is the typical uncertainty for shock tube IDT measurements in a CO_2 bath gas. UoS cCO_2 mechanism, which was initially developed using limited H_2 IDT data, significantly outperforms AramcoMech 2.0, a well-validated chemical kinetic mechanism across a range of conditions. The current work validates the performance of the UoS sCO_2 2.0 mechanism

300 across a range of equivalence ratios, pressures, and bath gas compositions for CO_2-diluted H_2 ignition.
301 This work also identifies areas of improvement for prediction H_2 ignition in CO_2 bath gas. This includes
302 measuring the reaction rate coefficient of Reaction 1 in CO_2 bath gas and IDT measurements at lower
303 temperatures. Another suggestion is to measure OH time-histories for H_2 combustion in CO_2 to validate
304 the mechanisms' ability in modelling the concentration of the most important radical of H_2 combustion.

305 ## 6. Conclusions

306 The present study investigates the combustion behaviour of H_2 in CO_2 bath gas by performing IDT
307 measurements of H_2 for various equivalence ratios and bath gas compositions at 20 and 40 bar. These data
308 fill the gaps in literature on experimental work of hydrogen IDTs in CO_2. Measured IDT data were used
309 to validate the UoS sCO_2 2.0 chemical kinetic mechanism which was developed recently to model the
310 combustion of methane, H_2, and syngas in CO_2 bath gas. UoS sCO_2 2.0 outperformed AramcoMech 2.0
311 in simulating IDT datasets as evaluated quantitively by comparing the average percentage difference
312 between the experimental and simulated IDTs. While there is still room for mechanism improvement as
313 identified by the sensitivity analysis and discussed in the present study, these data coupled with previous
314 works provide a wide-ranging validation platform for mechanisms to model IDTs of H_2 in CO_2 bath gas
315 over a wide range of conditions.

316 ## Acknowledgements

317 The work of KAUST authors was funded by baseline research funds at King Abdullah University of
318 Science and Technology (KAUST). The work of UoS was supported by EPSRC Centre for Doctoral
319 Training in Resilient Decarbonised Fuel Energy Systems (Grant number: EP/S022996/1) and the
320 International Flame Research Federation (IFRF).

321 ## Supplementary Material

322 This work contains supplementary material.

323 (Uncertainty of measured IDTs, Tables of measured IDTs, Mechanism files of UoS sCO_2 2.0).

References

[1] V. Masson-Delmotte, P. Zhai, A. Pirani, S.L., Connors, C. Péan, S. Berger, N. Caud, Y. Chen, L. Goldfarb, M.I. Gomis, M. Huang, K. Leitzell, E. Lonnoy, J.B.R., Matthews, T.K. Maycock, T. Waterfield, O. Yelekçi, R. Yu, B. Zhou, IPCC, 2021: Climate Change 2021: The Physical Science Basis. Contribution of Working Group I to the Sixth

Assessment Report of the Intergovernmental Panel on Climate Change, 2021.

[2] K.L. Ebi, J. Vanos, J.W. Baldwin, J.E. Bell, D.M. Hondula, N.A. Errett, K. Hayes, C.E. Reid, S. Saha, J. Spector, P. Berry, Extreme Weather and Climate Change: Population Health and Health System Implications, Annual Review of Public Health 42 (2021) 293-315.

[3] N. Höhne, M.J. Gidden, M. den Elzen, F. Hans, C. Fyson, A. Geiges, M.L. Jeffery, S. Gonzales-Zuñiga, S. Mooldijk, W. Hare, J. Rogelj, Wave of net zero emission targets opens window to meeting the Paris Agreement, Nature Climate Change (2021).

[4] R.J. Allam, M.R. Palmer, G.W. Brown, J. Fetvedt, D. Freed, H. Nomoto, M. Itoh, N. Okita, C. Jones, High efficiency and low cost of electricity generation from fossil fuels while eliminating atmospheric emissions, including carbon dioxide, GHGT-11 37 (2013) 1135-1149.

[5] NetPower, Home. https://www.netpower.com/ (accessed 7th November 2019).

[6] A. Rathi, U.S. startup plans to build first zero-emission gas power plants. https://www.bloomberg.com/news/articles/2021-04-15/u-s-startup-plans-to-build-first-zero-emission-gas-power-plants (accessed 15th April 2021).

[7] G. Kelsall, 8 Rivers Capital and Sembcorp Energy UK's first zero emissions power plant. https://ifrf.net/ifrf-blog/8-rivers-capital-and-sembcorp-energy-uk-to-develop-uks-first-net-zero-emissions-power-plant/ (accessed 2nd August 2021).

[8] R.J. Allam, J.E. Fetvedt, B.A. Forrest, D.A. Freed, The oxy-fuel, supercritical CO_2 Allam cycle: new cycle developments to produce even lower-cost electricity from fossil fuels without atmospheric emissions, Proceedings of the Asme Turbo Expo: Turbine Technical Conference and Exposition 3b (2014).

[9] J. Harman-Thomas, K.J. Hughes, M. Pourkashanian, The development of a chemical kinetic mechanism for combustion in supercritical carbon dioxide, Energy (2022) 124490.

[10] J.K. Shao, R. Choudhary, D.E. Davidson, R.K. Hanson, S. Barak, S. Vasu, Ignition delay times of methane and hydrogen highly diluted in carbon dioxide at high pressures up to 300 atm, Proceedings of the Combustion Institute 37 (2019) 4555-4562.

[11] M. Alabbad, Y. Li, K. AlJohani, G. Kenny, K. Hakimov, M. Al-lehaibi, A.-H. Emwas, P. Meier, J. Badra, H. Curran, Ignition delay time measurements of diesel and gasoline blends, Combustion and Flame 222 (2020) 460-475.

[12] M. AlAbbad, T. Javed, F. Khaled, J. Badra, A. Farooq, Ignition delay time measurements of primary reference fuel blends, Combustion and Flame 178 (2017) 205-216.

[13] A.S. AlRamadan, J. Badra, T. Javed, M. Al-Abbad, N. Bokhumseen, P. Gaillard, H. Babiker, A. Farooq, S.M. Sarathy, Mixed butanols addition to gasoline surrogates: Shock tube ignition delay time measurements and chemical kinetic modeling, Combustion and Flame 162 (2015) 3971-3979.

[14] J.W. Hargis, E.L. Petersen, Methane ignition in a shock tube with high levels of CO_2 dilution: consideration of the reflected-shock bifurcation, Energy & Fuels 29 (2015) 7712-7726.

[15] M. Karimi, B. Ochs, W. Sun, D. Ranjan, High pressure ignition delay times of H_2/CO mixture in carbon dioxide and argon diluent, Proceedings of the Combustion Institute (2020).

[16] H. Mark, The interaction of a reflected shock wave with the boundary layer in a shock tube, Cornell University, Ithaca, New York, United States, 1958.

[17] D. Bull, D. Edwards, An investigation of the reflected shock interaction process in a shock tube, AIAA Journal 6 (1968) 1549-1555.

[18] H. Kleine, V. Lyakhov, L. Gvozdeva, H. Grönig, Bifurcation of a reflected shock wave in a shock tube, Shock Waves, Springer1992, pp. 261-266.

[19] E.L. Petersen, Interpreting endwall and sidewall measurements in shock-tube ignition studies, Combustion Science and Technology 181 (2009) 1123-1144.

[20] M. Lamnaouer, A. Kassab, E. Divo, N. Polley, R. Garza-Urquiza, E. Petersen, A conjugate axisymmetric model of a high-pressure shock-tube facility, International Journal of Numerical Methods for Heat & Fluid Flow (2014).

[21] W.K. Metcalfe, S.M. Burke, S.S. Ahmed, H.J. Curran, A hierarchical and comparative kinetic modeling study of C1 − C2 hydrocarbon and oxygenated fuels, International Journal of Chemical Kinetics 45 (2013) 638-675.

[22] K.P. Grogan, M. Ihme, Regimes describing shock boundary layer interaction and ignition in shock tubes, Proceedings of the Combustion Institute 36 (2017) 2927-2935.

[23] Z. Hong, D.F. Davidson, E.A. Barbour, R.K. Hanson, A new shock tube study of the $H + O_2 \rightarrow OH + O$ reaction rate using tunable diode laser absorption of H_2O near 2.5 μm, Proceedings of the Combustion Institute 33 (2011) 309-316.

[24] S. Wang, D.F. Davidson, R.K. Hanson, Shock Tube and Laser Absorption Study of CH2O Oxidation via Simultaneous Measurements of OH and CO, The Journal of Physical Chemistry A 121 (2017) 8561-8568.

[25] J. Shao, Shock tube studies of hydrocarbon fuels at elevated pressures, Mechanical Engineering, Stanford University, Stanford, 2019.

[26] S.S. Vasu, D.F. Davidson, R.K. Hanson, Shock tube study of syngas ignition in rich CO_2 mixtures and determination of the rate of $H+O_2+ CO_2 \rightarrow HO_2+CO_2$, Energy & Fuels 25 (2011) 990-997.

[27] E. Hu, L. Pan, Z. Gao, X. Lu, X. Meng, Z. Huang, Shock tube study on ignition delay of hydrogen and evaluation of various kinetic models, International Journal of Hydrogen Energy 41 (2016) 13261-13280.

[28] J. Shao, R. Choudhary, D.F. Davidson, R.K. Hanson, S. Barak, S. Vasu, Ignition delay times of methane and hydrogen highly diluted in carbon dioxide at high pressures up to 300 atm, Proceedings of the Combustion Institute 37 (2019) 4555-4562.

[29] B.A. Ellingson, D.P. Theis, O. Tishchenko, J. Zheng, D.G. Truhlar, Reactions of hydrogen atom with hydrogen peroxide, The Journal of Physical Chemistry A 111 (2007) 13554-13566.

[30] W. Tsang, R.F. Hampson, Chemical kinetic data base for combustion chemistry. Part I. Methane and related compounds, Journal of Physical and Chemical Reference Data 15 (1986) 1087-1279.

[31] Y. Wu, S. Panigrahy, A.B. Sahu, C. Bariki, J. Beeckmann, J. Liang, A.A. Mohamed, S. Dong, C. Tang, H. Pitsch, Understanding the antagonistic effect of methanol as a component in surrogate fuel models: A case study of methanol/n-heptane mixtures, Combustion and Flame 226 (2021) 229-242.

[32] M.F. Campbell, T. Parise, A.M. Tulgestke, R.M. Spearrin, D.F. Davidson, R.K. Hanson, Strategies for obtaining long constant-pressure test times in shock tubes, Shock Waves 25 (2015) 651-665.